Defence Science Journal, Vol. 70, No. 2, March 2020, pp. 122-130, DOI : 10.14429/dsj.70.12788

Analysis of a Compact Squeeze Film Damper with Magneto-Rheological Fluid

Rahul K. Singh, Mayank Tiwari*, Anpeksh A. Saksena, and Aman Srivastava

Indian Institute of Technology Patna - 801 106, India
**E-mail: mayankt@iitp.ac.in*

ABSTRACT

Rotor systems play vital role in many modern day machinery such as turbines, pumps, aeroengines, gyroscopes, to name a few. Due to unavoidable unbalance in the rotor systems, there are lateral and torsional vibrations. Ignoring these effects may cause the system serious damages, which sometimes lead to catastrophic failures. Vibration level in rotor systems is acceptable within a range. Focus in this work is to minimize the vibration level to the acceptable range. One of the ways vibration level can be minimised is by means of providing damping. To accomplish this task in this work a new concept squeeze film damper is made by electro discharge machining which is compact in configuration, is filled with magneto-rheological (MR) fluid and tested out on one support of a Jeffcott rotor. This compact squeeze film damper (SFD) produces damping in a compact volume of the device compared to a conventional SFD. MR fluid is a smart fluid, for which apparent viscosity changes with the application of external magnetic field. This compact damper with MR fluid provides the variable damping force, controlled by an external magnetic field. In this work, proportional controller has been used for providing the control feedback. This MR damper is seen to reduce vibrations in steady state and transient input to the Jeffcott rotor. Parametric study for important design parameters has been done with the help of the simulation model. These controlled dampers can be used for reducing vibrations under different operating conditions and also crossing critical speed.

Keywords: Rotor; Squeeze film damper; Magneto rheological fluid; Vibration control; Ball bearing

NOMENCLATURE

μ	Magnetic permeability of free space
μ_r	Relative permeability
B	Magnetic flux density
η	Dynamic viscosity
C,	Damping Coefficient
K,	Stiffness of shaft
M, m	Mass
F_{unb}	Unbalance Force
F_d	Damping force
X, x, Y, y	Displacement
Ω	Rotational speed
ω_n	Natural frequency
T	Damper plate thickness
c_1	Damping land clearance
c_2	Clearance between damper plate and end plate
l_1	Flow length
R_1	Radius of damping land
R_2	Radius of the 'O' ring seal
τ_y (H)	Yield stress
T	Shear stress
H	Magnetic field intensity
δ	Logarithmic decay rate
ζ	Damping ratio

Received : 11 March 2018, Revised : 08 January 2020
Accepted : 19 February 2020, Online published : 09 March 2020

1. INTRODUCTION

The motivation for this work comes from the need for a compact and effective method of vibration control of rotors, like a compact squeeze film damper with active control. A squeeze film damper (SFD) reduces the dynamic load, which is transmitted to the bearings and can help to reduce the sensitivity to change in unbalance. A conventional SFD with squirrel cage, specially centralised SFD occupies space in the axial direction is unpredictable many times due to nonlinearity and is not compact.

SFD has been used for over four decades in order to limit the vibration amplitude of rotor due to residual unbalance. A good review by Della[1], *et al.* has been done on the Squeeze Film Damper and its development through the years. The major drawback of conventional SFD is its non-linearity of damping which nullifies the expected benefit. To counter these problems and make the squeeze film damper more controllable and predictable Walton & Heshmat[2], presented a multi squeeze film damper (MSFD), in which within the clearance a single wrap of an Inconel spiral thin foil was inserted in a squeeze film damper, its ends attached to the damper journal and to the ring. Zeidan[3], *et al.*, and De Santiago[4], *et al.* proposed and experimented an integral squeeze film damper (ISFD). With respect to conventional design, the new proposed design of the squeeze film damper has a substantial reduction in its axial dimensions.

Work by Ertas[5], *et al.*, on power turbines show that ISFD improves the stability margin by a factor of 12, eliminates the sub-synchronous instability and significantly reduces amplification factors at critical speeds. Moreover, by using ISFD the analysis shows a significant fall in inter-stage clearance closures during critical speed transitions in contrast to the hard mounted tilting pad bearing configuration. Heidari[6], *et al.* have presented a theoretical model for an active squeeze film damper (ASFD) as an option in the vibration control field. The design is based on the conventional SFD with the controllability characteristics of magnetic bearing, which allows the development of a variable force, and a change in fluid film stiffness and damping.

From the above it is seen that most work done is on conventional SFD however ISFD as a compact and linear damper for rotors with journal bearings has been studied previously by Zeidan[3], *et al.* De Santiago[4], *et al.* and Ertas[5], *et al.* proposed compact SFD has similar features but with different configuration. In this work, a compact SFD is used with ball bearing with a smart fluid (MR Fluid), used as a viscous medium. This MR fluid controlled damper for such configuration is not yet reported in literature.

2. COMPACT SQUEEZE FILM DAMPER

Similar to the compact design used for ISFD for fluid film bearings by Ertas[5], *et al.*, in this work a compact SFD is made for mounting ball bearings (Figs. 1(a) and 1(b)). Unlike conventional SFD, which have a 2π film of fluid, the new partitioned compact SFD fabricated by Srivastava[6] does not allow any type of flow over the circumference and offers a different circumferential boundary condition for the film flow domain.

The method for damping used in the compact SFD is ruled by piston/dash-pot damping, similar to ISFD, which is generated through fluid flow resistances at damping land and end seals. So logically the important design parameters of the compact SFD are the clearance of damping land and end seal clearances. Parametric analysis of this design is done in this work. This new design approach for energy loss using orifice "dashpots" and end seal provides a linear system which has less film cavitation and so produces damping force over a wider operating range[5]. The difference between conventional SFD with squirrel cage and the compact SFD technology is the EDM (electric discharge machining) manufacturing process which allows for single integrated bearing damper. This damper has two pieces: (1) outer rim and (2) inner rim, both machined from a single piece. The outer rim and inner rim are mechanically coupled with the help of eight EDM machined integral spring, which provides the radial static stiffness coefficient for the bearing support (Fig. 1(a)-1(b)) also the bearing houses in the inner rim. In the compact SFD when whirling of rotor takes place, S-shaped spring store the energy and transmit it to the damping land. The damping land squeezes the fluid, which flows through clearance provided with end plates. The damping force is generated due to viscous flow of fluid in damping land and in the clearance between end plate and damper plate.

2.1 Mathematical Modelling of the Compact SFD

In the damping land fluid volume provides damping due to flow in the thin 'channel'. The cross-sectional area of the flow out of the damper land is A_i equal to $R_1\theta c_1$ (length of damping land * clearance), where R_1 is inner radius of damping land shown in Fig. 1(a) and (b) and θ is the angle made by ends of damping land (sector), Fig. 1, from the center of the damper. When the damping land squeezes, it will force the fluid to flow through damping land and channel (clearance) in end plates, damping will be provided by fluid flow resistance. There are two passages for fluid flow one on left and right side of damper plate.

Both end plates are identical in geometry. End plate and damper plate have clearance C_2 up to length l_1. Damper plate thickness is denoted by t and damping land has clearance C_1, (Fig. 1 b). To derive damping force due to viscous flow, it is necessary to understand the geometry of channels through which fluid will flow. Geometry can be divided in two section, each section is identical in geometry.

In the damping land area of channel is $R_1\theta c_1$ and effective length of channel is t i.e. thickness of damper plate. End plate will provide clearance c_2 for fluid flow so cross sectional area for fluid in end plate will be $\pi R_1 c_2$, however in end plate radius is not constant in the direction of fluid flow, it is changing from

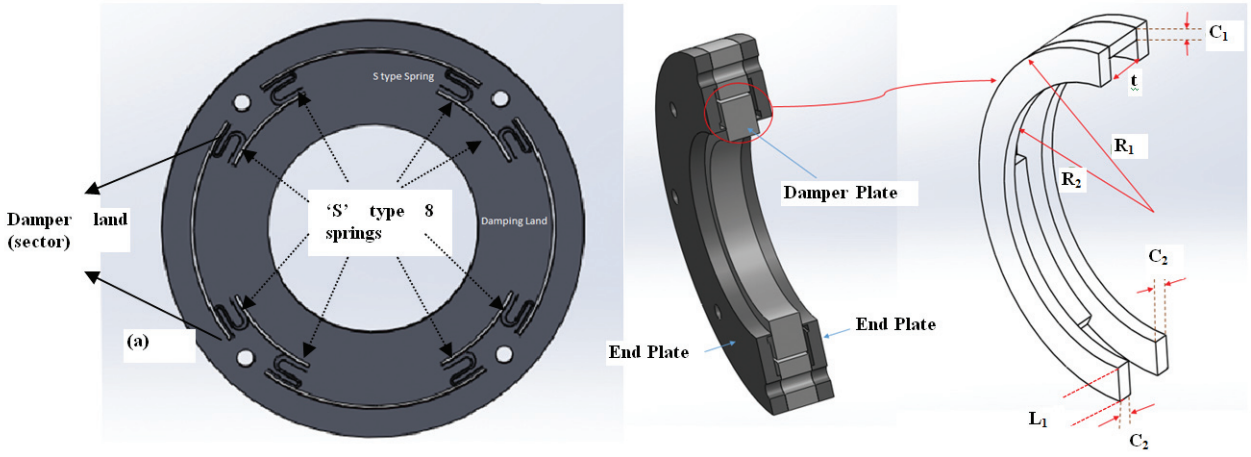

Figure 1. (a) Damper plate (b) Cross sectional view of damper assembly and damping land and fluid channel.

R_1 to R_2 so average of radius (R_1+R_2)/2 is taken, thus effective area will become $\pi(R_1+R_2)c_2$. Clearance has been provided in end plate over l_1 length. From Fig. 4, channel of section 1 and 2 are in are identical so Q_1 and Q_2 will be same i.e. $Q_1 = Q_2 = Q$,

Applying the Hagen–Poiseuille model (Singh[7], *et al.*) damping coefficient C_d can be written as[14]

$$C_d = 128\eta\left(\frac{t/2}{R_1\theta c_1} + \frac{l_1}{\pi(R_1+R_2)c_2}\right)R_1\theta t \quad (1)$$

From Eqn. (1) damping varies inversely with C_1, the damping land clearance, due to squeeze effect. Lower bound of $C_1$is determined by the EDM wire diameter and also the maximum rotor motion which can result in damper closing and introducing nonlinear effects also called 'bottom out' of damper.

2.2 Parametric Analysis of compact SFD for Damping Coefficient

Parametric analysis has been done for Eqn. (1) with numerical values η- dynamic viscosity of fluid is 0.112 Pa-s, t-thickness of damper plate is 5 mm, C_1- damping land clearance is 1 mm, C_2- clearance between end plate and damping land is 0.25 mm, l_1-effective length of clearance C_2 is 14 mm (l_1=C_1-C_2) , R_1-radius at which at which C_2 starts is 51 mm, R_2 Radius at which C_2 ends (O ring groove) is 37 mm, θ is angle made by one damping arc is 52°.

From this parametric analysis it is seen that the generated damping is linear with respect to the viscosity of the fluid, thickness of the damper plate (width of the damper 'piston') and flow length between the end plate and damper plate.

It is nonlinear with respect to damping land clearance and clearance between the end plate and damper plate. Damping land clearance is limited by the diameter of the EDM wire and also minimum amount for damper closure during high whirl amplitude of the rotor. Minimum gap between damper plate and end plate depends on the sealing configuration (O-ring diameter)

3. MAGNETO RHEOLOGICAL FLUID

AMT- DAMPRO MR Fluid by Falcon MR Tech Limited, India has been used in this compact SFD. The relationship for the dynamic viscosity in Pa-s and magnetic field B in tesla (T) is given by the Eqn. (2)

$$\eta = -2908*B^5 + 6422*B^4 - 5611*B^3 + 2338*B^2 + 49.62*B + 1.736 \quad (2)$$

It is linearised about 0.00157 *T* since the maximum magnetic field for this work can be 0.002512 *T* (limitations of number of coils and current as used in the experiments, explained later). Using Taylor series about 0.00157 *T* we get dynamic viscosity as function of magnetic field

$$\eta = 56.92*B + 1.731 \quad (3)$$

4. ANALYSIS OF ROTOR SYSTEM AND CONTROLLER DESIGN

From the equation of motion (Eqn. (4)) of a rotor system transfer function of rotor system has been derived. For a symmetrical Jeffcott rotor, there are negligible gyroscopic below the first critical speed so 1-DOF of the rotor is considered, i.e. vibration in one orthogonal direction to the rotational axis. In this simulation gyroscopic effect has not been considered. Equation of motion for 1-DOF rotor system is

$$M\ddot{x} + C_d\dot{x} + Kx = F_{unb} \quad (4)$$

$$F_{unb} = me\omega^2 \sin\omega t \quad (5)$$

where *M* is mass of disk, C_d damping coefficient, *K* is stiffness, m is unbalance mass, *e* is a distance of the unbalance mass from the center of the disk and ω is the angular velocity of the rotor.

Laplace transforms of Eqn. (4), assuming zero initial conditions

$$\frac{X(s)}{F(s)} = \frac{1/M}{s^2 + \frac{C_d}{M}s + K/m} \quad (6)$$

K/M is equal to square of natural frequency of rotor system and for analysis natural frequency (ω_n) is 26 Hz. *C/M* is equal to $2\varsigma\omega_n$, where ζ is damping ratio of rotor system[13].

Other parameters, based on the experimental data, used in simulation are: mass of disk *M* = 2.88 Kg, unbalance mass *m* = 0.015 Kg, eccentricity *e* = 50 mm from center of the disk, rotational speed 150 rad/s. The damping ratio due to structural damping of the system is a low value of 0.02. This is the value of damping ratio when the damper has no oil. To observe the transient response of the rotor system an impulse excitation is applied with sinusoidal input $\omega = 150 rad/s$. These impulse excitations could be representative of impulse/shock load on rotors.

4.1 Controller Design and Analysis

C_d is damping coefficient and it depends on the viscosity of fluid inside the damper, viscosity of MR fluid is dependent on magnetic field applied across the damper. Magnetic field across the damper can be controlled by varying the current in the coil. So, according to the vibration levels current should be applied into the coil to apply the adequate damping force for containing the rotor vibrations. The damping force can be written as Eqn. (7)

$$F_d = C_d\dot{x} \quad (7)$$

where C_d is the function of viscosity of fluid inside the damper.

$$C_d = kf(\mu) \quad (8)$$

k is the proportionality constant and depends on geometry of damper. From Eqn. (1)

$$C_d = 128\eta*\left(\frac{t/2}{R_1\Theta C_1} + \frac{l_1}{\Pi(R_1+R_2)C_2}\right)R_1\Theta t \quad (9)$$

From Eqns. (8) and (9)

$$k = 128*\left(\frac{t/2}{R_1\Theta C_1} + \frac{l_1}{\Pi(R_1+R_2)C_2}\right)R_1\Theta t \quad (10)$$

Substituting value of the parameters in Eqn. (10)

$k = 10.1081$

Equation (7) is then

$$F_d = 10.1081\eta\dot{x} \quad (11)$$

From Eqn. (3)

$$F_d = 10.1081*(56.92*B+1.731)\dot{x} \quad (12)$$

For this simulation, magnetic flux (tesla) generated is

$$B = \frac{\mu NI}{2r} \quad (13)$$

here N is the number of turns on solenoid, r is the radius of the circular loop of solenoid coil, μ is the magnetic permeability of free space. In the experimental setup N = 60 turns, the value of I, current, is variable. Value used in simulation are same as of actual experimental setup. Control logic is implemented to control the vibration of the rotor system given in Fig. 2.

Structural and viscous damping has been considered, of which, structural damping is constant. Viscous damping is variable depending on magnetic field. In the Simulink model, Fig. 2, sinusoidal input is given to the system. At t = 5 s impulse of 20 unit has been added to observe the transient response. This analysis was done at rotational speed of 150 rad/s. Two cases were analysed, in the first case there is no control logic, damping provided to the system is structural damping (ζ=0.02). In the second case control logic is implemented with a proportional controller (gain k=20). In this analysis, Fig. 3, it was found that with the control logic vibration amplitude level has been reduced also as the control was implemented the waveform achieves its steady state faster with almost no transient envelope of the response.

4.2 Parametric Analysis of the Compact SFD

The design parameters of the compact SFD are varied in defined ranges and effect on response of the rotor system studied. For this the Simulink[9] model developed for open loop with unbalance force is used for analysis.

From the parametric runs, Fig. 4 it is observed that if damper plate thickness is more it introduces more damping. This is logical since increase in plate thickness increases area of damper (piston). For less thickness damping is negligible. On the other hand smaller dimensions of C_1- damper land clearance and C_2- end plate clearance gives rise to higher damping. Also for very small C_1 and C_2 response is very sensitive to these clearance values. Following conclusion can be made from Fig. 4.

- Damping land clearance should have minimum value for higher damping. But if damping land clearance is very small then 'bottom out' will occur for high rotor amplitudes which results in nonlinear stiffness of 'S' shaped spring
- Clearance between end plate and damper plate should be as small as possible for higher damping, higher clearance will result in low damping.
- Damper plate thickness should be high. But if damper plate thickness is high it will increase the stiffness of the 'S' spring.
- Flow length should be high, although this is the parameter on which response has least sensitivity

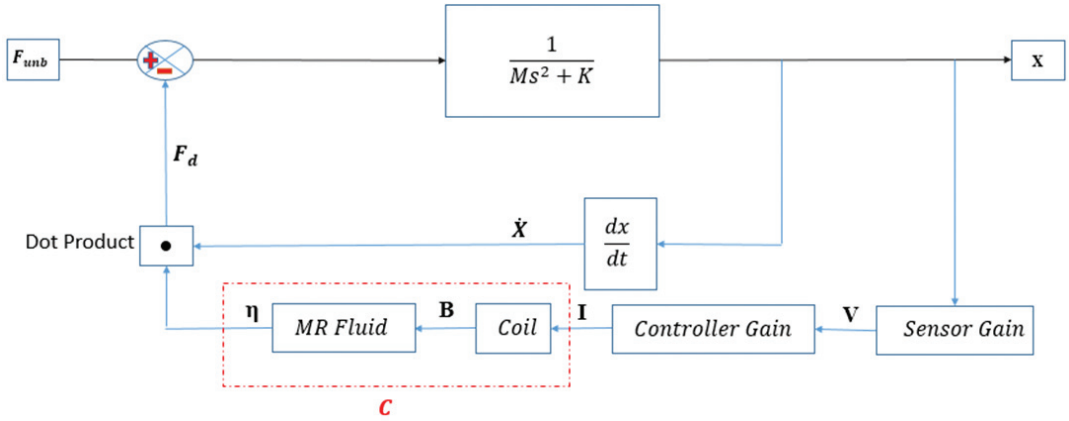

Figure 2. Control logic in SIMULINK[9].

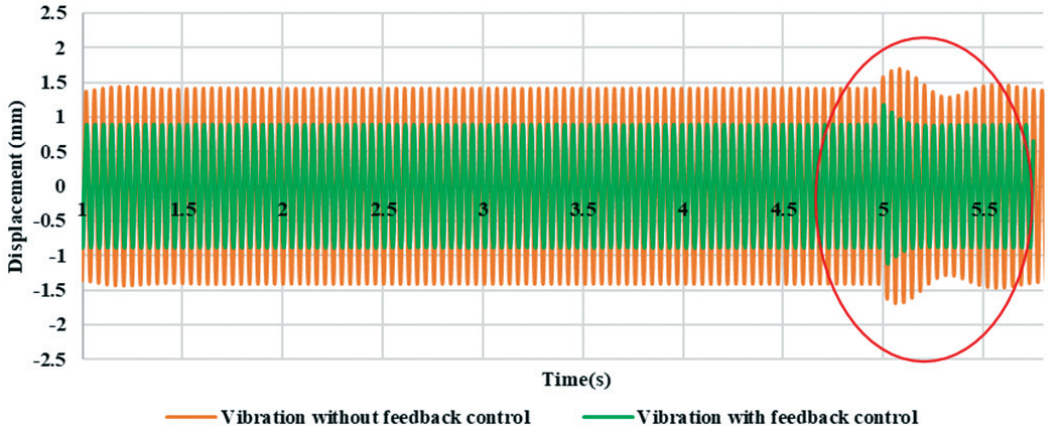

Figure 3 Simulation: Response to impulse excitation of rotor system.

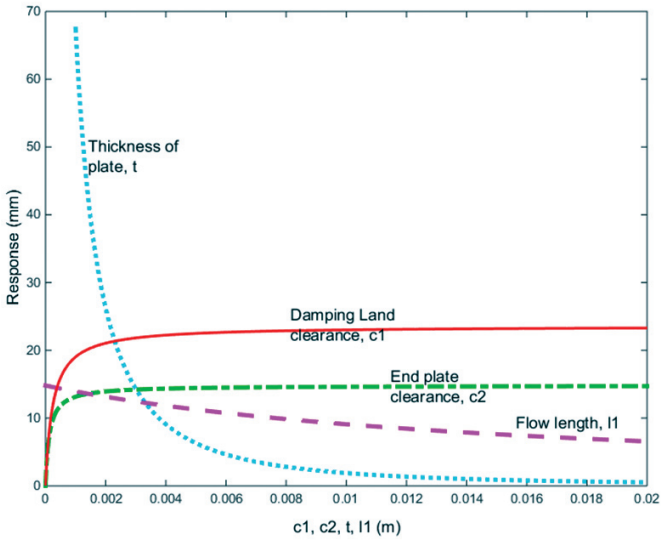

Figure 4 Response vs. design parameters.

5. EXPERIMENTAL SETUP

5.1 Rotor System

To study the lateral vibration of rotor caused by rotor unbalance, a rotor system was fabricated by Saksena[8]. It consists of a shaft of diameter (d) 20 mm and length 1000 mm, having a disk at the center of shaft. Mass of the disk is 2.88 Kg. Below is a list of components of the rotor system.

i. Mild steel disc of diameter 150 mm with collars for locks, and thickness 20 mm.
ii. Mild steel shaft of diameter 20 mm and length of 1000 mm.
iii. 58 1HP 24 Volt DC- BLDC Motor by Tachometric Controls.
iv. Two SKF 6004 bearing.
v. Coupling for connecting motor to the shaft and two bearing housings.
vi. 250 ml of MR Fluid (FALCON MR-TECH)
vii. DC power supply of 720 W, Max voltage 36 V and maximum current 20 A.

The rotor has been designed using KISSsoft[10], Fig. 5. The compact SFD is as shown in Fig. 6. To control the viscosity of MR fluid with the help of external magnetic field, two solenoid plates were placed with copper wire winding over it, and damper is situated in between the solenoid plates. (Fig. 7) The solenoid plate has copper wire winding over it. Two proximity probe (inductive type) are used for measurement of vibration of shaft (in terms of displacement) in x and y-orthogonal directions.

6. EXPERIMENTAL ANALYSIS AND RESULTS

6.1 Impulse (Impact Hammer) Test

In impact hammer tests, an impulse was applied to the rotor system. Multiple impact hammer test on rotor system were carried out to identify natural frequency, structural damping of

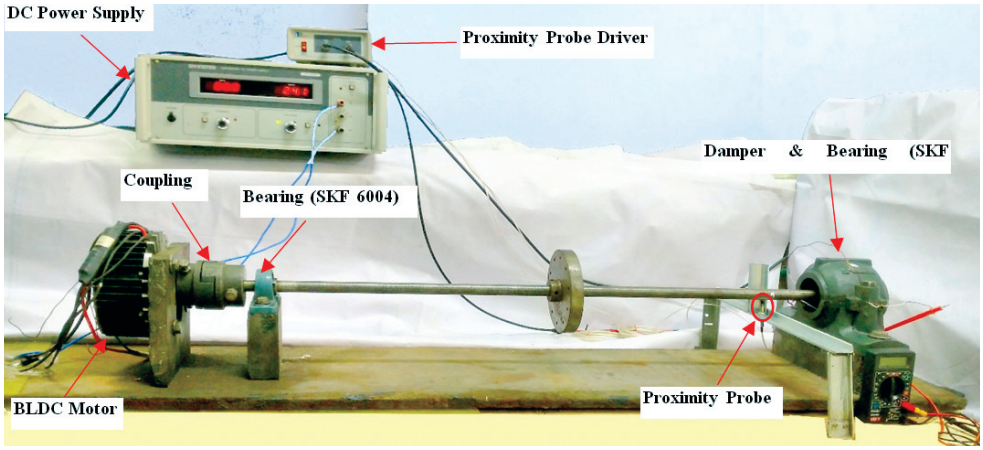

Figure 5. Test rotor system.

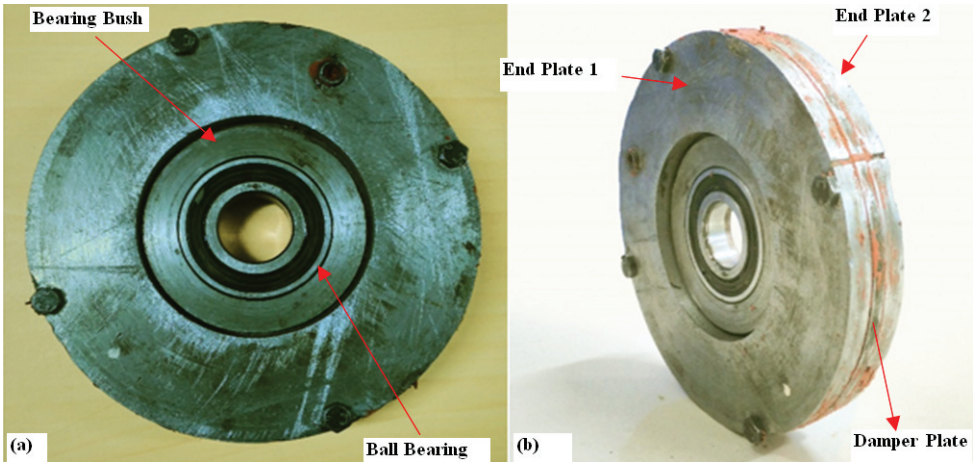

Figure 6. Actual damper assembly (a) Front view (b) side view.

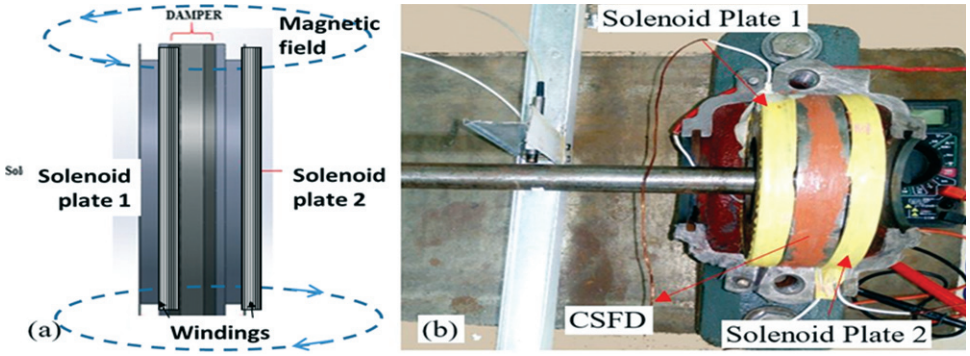

Figure 7. Solenoid and damper plate (a) schematic (b) Actual assembly.

rotor and viscous damping of damper as well. To conduct these experiments a Bruel & Kjær's impact hammer with load cell tip, Polytec PDV Laser Vibrometer, Data Acquisition System, Vibsoft Software (vibration analyser) are used.

6.2 Natural Frequency Test

Verification of theoretical natural frequency has been done using an impact hammer test. In this experiment, rotor system has been excited with an instrumented impact hammer impulse at the disk.

The natural frequency obtained from the experiment was 27.91 Hz. Calculated natural frequency is 25.84 Hz without damper. The small difference can be attributed to different end conditions on the bearings in theory and experiment.

6.3 Estimation of Damping

Impact hammer test has been carried out on a stationary rotor, to find the structural damping of the rotor system and viscous damping of the damper as well. This test was performed with different damper system configuration.

6.3.1 Case I: Damping Test without Oil

To find out the structural damping of the rotor system damper is not activated, i.e. there was no oil in damper. An impact hammer, at the disk, excited rotor system and response of rotor in terms of velocity was recorded by laser Vibrometer. Velocity amplitude with respect to time has been plotted in Fig. 8. Velocity amplitude decay curve with almost linear envelope shows that there is structural damping (non-viscous[13]) in the rotor system.

6.3.2 Case II: Damping Test with Oil

To investigate about the viscous damping of damper, it was activated, i.e. filled with Gear Drive oil with viscosity 90 cst. The rotor was excited by an impact hammer at the disk location and vibration amplitude in terms of velocity was recorded by vibrometer.

This experiment was performed to investigate level of viscous damping provided by this damper. As can be seen in Fig. 8, with oil, the oscillations start with higher amplitude than without oil but reach the same value in the same time- which is due to greater damping. Oscillation with oil, attenuate sooner than without oil. This indicates that with damper with oil has damping consisting of viscous damping and structural damping.

6.3.3 Case III: Damping Test with MR Fluid

From case II results, it has been verified that damper is providing viscous and structural damping both. To provide variable damping force to the system, MR fluid is now filled in the damper. This experiment was performed at 0 A, 2 A and 4 A current. From Fig. 9 it is observed that on application of variable magnetic field, variable damping force can be obtained. As the magnetic field increased damping of the system also increased.

From Fig. 9(a) MR fluid with 2 A current in coil has more damping than 0 A current. Similarly from Fig. 9(b) MR fluid with 4 A current in coil has more damping than previous two experiments. It can be seen from the Fig. 3 that curve with higher damping characteristics, requires less time to reach the steady state value.

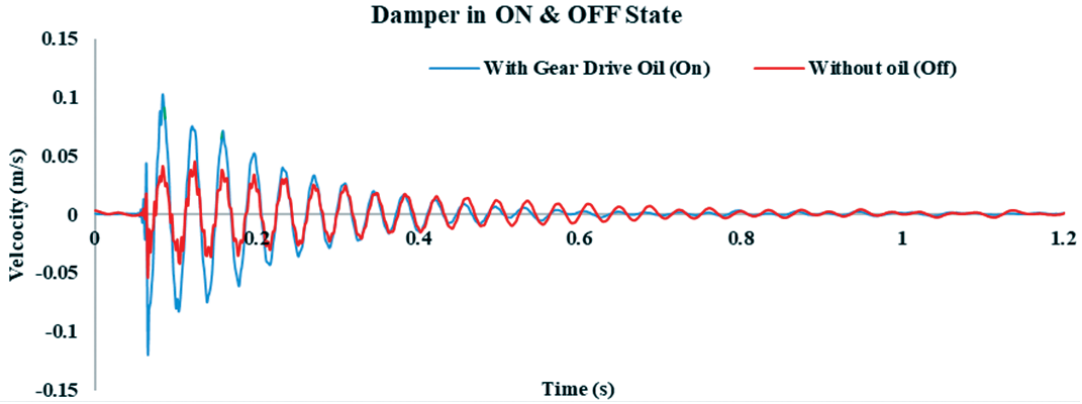

Figure 8. Response of rotor for impact hammer test on stationary rotor.

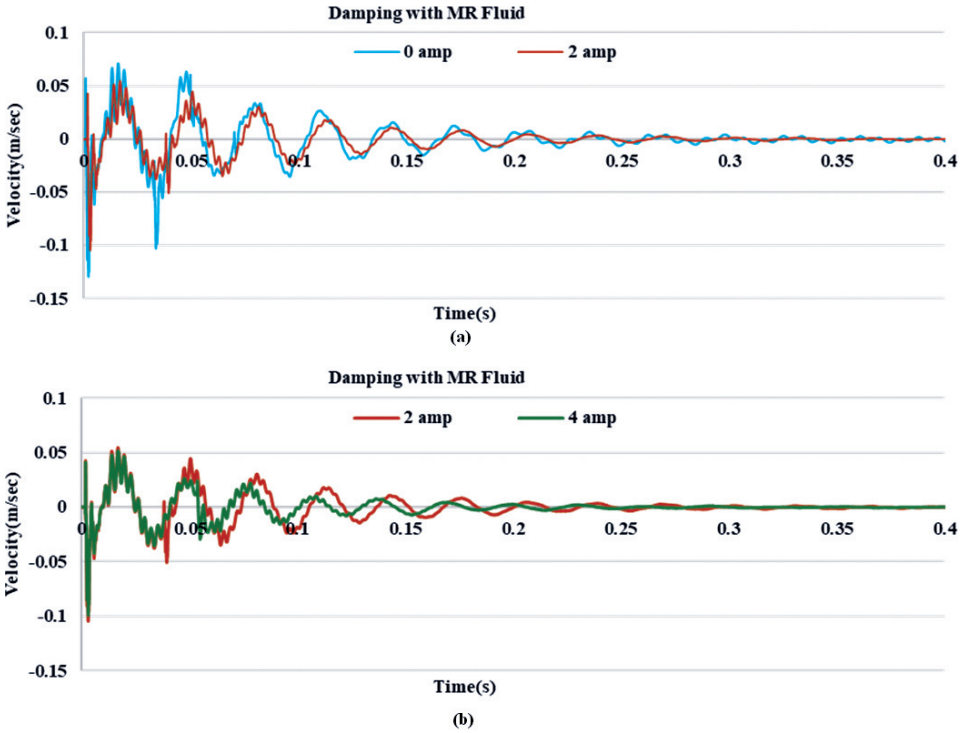

Figure 9 Impact hammer test with MR fluid (a) 0 amp and 2 amp (b) 2 amp and 4 amp current.

Damping ratio ζ can be calculated from Figs. 8 and 9. Logarithmic decrement δ is given by[13]

$$\delta = 2\pi\zeta \tag{14}$$

Case I, II and III results are compared in Table 1

Table 1. Damping ratio calculated from experimental results

Description		ζ
Case I: without oil		0.02
Case II: with gear drive oil		0.04
Case III: MR fluid	0 amp current into the coil	0.045
	2 amp current into the coil	0.06
	4 amp current into the coil	0.09

6.4 Measurement of Vibration Amplitude and It's Control

Feedback control has been implemented to provide variable damping force in the rotor system (Fig. 2). Proportional controller was used to control vibration level. After receiving information from sensor, the Arduino sends PWM control signal to the driver circuit. According to the PWM signal, driver applies voltage across the coil, which results in the magnetic field generation, and this magnetic field changes the viscosity of MR fluid. Variable viscosity of MR fluid provides variable damping to the system. This experiment was performed at a speed of 550 RPM. There are two sensors placed orthogonally on the shaft for signals from X and Y directions. To obtain transient response of the system, impulse input was applied through a hammer by impacting the rotor at the disc, while it was rotating in this low speed.

Single plane balancing of the rotor was done before performing this experiment. Before balancing vibration amplitude in terms of velocity was 989 mm/s at 520 RPM, after balancing the rotor this amplitude is reduced to 147 mm/s.

Case I: Response of rotor without control

MR fluid is operated in off state with gain = 0

Case II: Response of rotor with controller gain 1

In this experiment controller gain was increased (doubled) to 1. At this gain maximum current into the coil will be 4 amp. Response of rotor running at 550 RPM after increasing the gain, displacement in x is reduced from 0.41 mm to 0.31 mm, and displacement in y is reduced from 0.45 mm to 0.36 mm as shown in Fig. 10.

To analyse the transient response of rotor impulse input

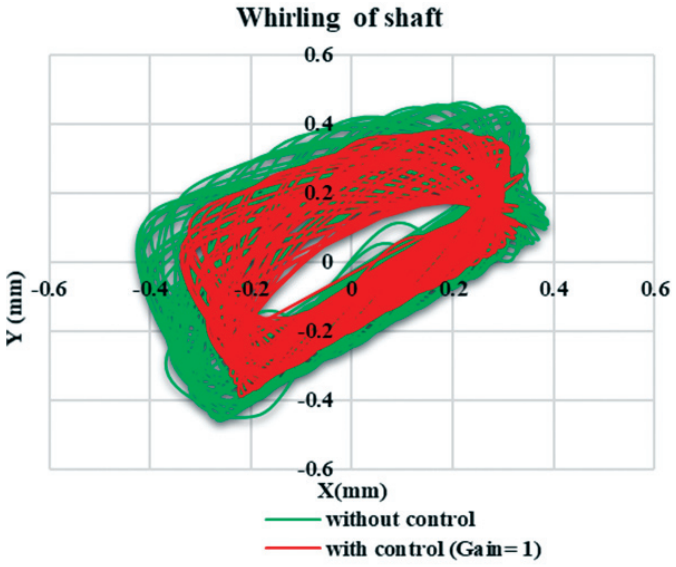

Figure 10. Comparison of rotor response at gain 1 and at gain 0 (without control).

was applied through hammer impact on disk in y direction, for a rotor running at 550 RPM as shown in Fig. 11.

Due to impulse input of the hammer vibration amplitude was increased, and it returns to its steady state value. If there is no controller system will take more time to return to its steady state. But on application of controller this transient time is reduced. It can be seen from Fig. 11, with controller, transient response to the impulse input is decreased. This compares well with the trend in theoretical results as shown in Fig. 3.

6.5 Comparison of Analytical and Experimental Results

From experimental results it is seen that for 550 RPM at sensor position i.e. 185 mm from damper end

i. Without controller whirl maximum displacement in X and Y directions are 0.41 mm and 0.46 mm.
ii. With controller (gain=1) whirl maximum displacement in X and Y directions are 0.31 mm and 0.36 mm.

To find out the maximum displacement due to unbalance at disk location beam bending equations considering Euler beam, have been used for simply supported beam bending under a force (unbalance) at the middle of the beam.

$$D_{disk} = 1.719 * D_{sensor} \quad (15)$$

From the above equations the experimental whirl amplitude in X and Y directions at the disk location,

i. Without control is 0.704 mm and 0.79 mm, respectively.
ii. With control it is 0.53 mm and 0.61 mm, respectively.

Theoretically the unbalance response of rotor is calculated based on a single degree of freedom model with no gyroscopic and well below the first critical[13]. At unbalance of 0.014 kg-m with controller gain 1 ($\zeta = 0.1$) displacement in X and Y should be 0.68 mm (circular whirl orbit radius).

So, while analytically we find the displacement in X and Y to be 0.68 mm respectively , experimentally it comes out to be 0.53 mm and 0.61 mm in X and Y respectively.

From above, it is seen that experimental result are close but less than analytical result due to end conditions actually being between simply supported and fixed, also possibly due to

i. Sensor error and data acquisition error due to interference of AC signal.
ii. Error in linearisation of the mathematical expression of MR fluid viscosity.
iii. Modelling the rotor as a one degree of freedom system is an assumption which contributes to the difference and will be taken care of in the future work.

7. CONCLUSIONS

A compact SFD has been fabricated based on damper design reported before by Zeidan[3], *et al.*, De Santiago[4], *et al.* and Ertas[5], *et al.*. Different from previous reported literature a ball bearing with MR fluid is used in this SFD. The major manufacturing process for this SFD has been EDM. A damping model for this SFD has been made considering flow of liquid through the SFD clearances and flow paths. From the model it can be seen that the damping generated is mostly linear with these parameters except for damping land clearance and clearance between plates. This model is used in defining the damping and used for a single degree of freedom model of a Jeffcott rotor, with centrally placed disc. The rotor is analysed for this damping, stiffness and mass values for a centrally placed disc running at speeds less than 50 % of first critical for which gyroscopic effects are negligible. With negligible coupling between X and Y radial directions, single degree of freedom model for X and Y is used for simulating in MATLAB and Simulink[9]. The model is used for a parametric study of damping land clearance C_1, endplate-damper plate clearance C_2, flow length l_1 and thickness of plate 't'. This study shows that end clearance (between damper plate and endplate) and land clearance (determined by EDM process) and thickness of the damper plate are very important for generating effective damping. This model is used for developing a proportional feedback controller with control of damping. MR fluid viscosity for different current (magnetic field) is linearised and

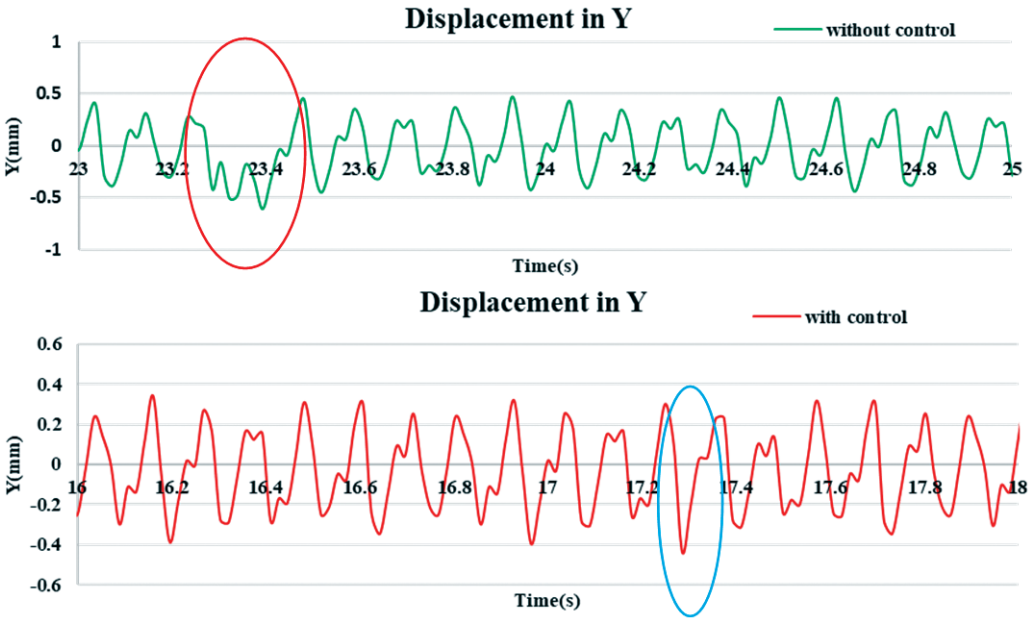

Figure 11. Impulse response of the rotor.

included in this model. From experimental results it was found that proposed compact SFD damper can reduce the vibration of rotor. Integration of damper and bearing into single unit makes it compact in size. Due to its compact size it requires lesser space than conventional SFD. Using MR fluid with proposed compact SFD increases its effectiveness. It can be seen from the experimental results that dynamic characteristics of rotor can be easily controlled by the application of external magnetic field. With MR fluid variable damping force can be provided to the system without changing the dimensions of damper. Dynamic characteristics of damper can be controlled by simply changing the current into the coil. This compact SFD with MR fluid is effective in controlling the vibration. For both transient (impulse) loading the feedback control reduced transients. This was seen from the theoretical model and also experimental results. Similarly for steady state conditions by changing the control gain the rotor vibrations could be reduced. The theoretical results are close to experimental results.

Clearance between end plates and damper plate should be as low as possible (Fig. 4), to increase the damping capability of damper. The damping land clearance should be small, as it determines squeeze film damping, however EDM wire diameter and also maximum rotor motion determines the lower bound on this. Ongoing work is investigating various topologies of the damper.

REFERENCES

1. Della Pietra, L. & Adiletta, G. The squeeze film damper over four decades of investigations. Part I: Characteristics and operating features. *Shock Vib. Dig*., 2002, **34**(1), 3-26.
2. Walton, J. & Heshmat. H. Rotordynamic evaluation of an advanced multisqueeze film damper—imbalance response and blade-loss simulation. *J. Eng. Gas Turbines Power,* 1993, **115**(2), 347-352. doi:10.1115/1.2906715
3. Zeidan, F.Y.; San Andres, L. & Vance, J.M. Design and application of squeeze film dampers in rotating machinery. *In P*roceedings of the 25th Turbomach. Symposium,1996.
4. De Santiago, O.; San Andrés, L. & Oliveras, J. Imbalance response of a rotor supported on open-ends integral squeeze film dampers. *J. Eng. Gas Turbines Power,* 1999, **121**(4), 718-724. doi:10.1115/1.2818532
5. Ertas, B.; Vaclav, C.; Joongsoo, K. & Vaclav, P. Stabilizing a 46 MW multistage utility steam turbine using integral squeeze film bearing support dampers. *J. Eng. Gas Turbines Power*, 2015, **137**(5), 052506-052506-11. doi:10.1115/1.4028715
6. Heidari, H.R. & Safarpourb. P. Design and modeling of a novel active squeeze film damper. *Mech. Mach. Theory,* 2016,**105**, 235–243. doi:10.1016/j.mechmachtheory.2016.07.004
7. Srivastava, A. Optimization of vibration in rotors. IIT Patna, Patna, 2015. (BTech Thesis).
8. Singh, R.; Kim, G. & Ravindra, P. Linear analysis of automotive hydro-mechanical mount with emphasis on decoupler characteristics. *J. Sound Vib.,*1992, **158**(2), p. 219-243. doi:10.1016/0022-460X(92)90047-2
9. MATLAB and Statistics Toolbox Release 2014b, The MathWorks, Inc., Natick, Massachusetts, United States
10. Saksena, A. Analytical and experimental analysis of a rotordynamic system with integral squeeze film damper. IIT Patna, Patna, 2016. (BTech Thesis).
11. KISSsoft 2015, KISSsoft AG-A Gleason Company,Zurich, Switzerland
12. Verma, H.C. Concept of physics, Part 2. Bharati Bhawan Pub. & Dis.,India.
13. Thomson, W.T.; Dahleh, M.D. & Padmanabhan, C. Theory of vibration with applications, Pearson, 2008.
14. Singh, R.K. Vibration control of rotor using a compact SFD with Magneto-rheological fluid. IIT Patna, Patna, 2016. (MTech Thesis).

CONTRIBUTORS

Mr Rahul K. Singh has obtained his MTech (Mechanical Engineering) from Indian Institute of Technology Patna, in 2017.

In the current study, he has performed all the experiments and validated the theory with experimental results. He is responsible for implementation of proportional gain controller based control system to limit the vibration of the rotor.

Dr Mayank Tiwari obtained his PhD from Indian Institute of Technology (IIT) Delhi and further did Post Doctorate from Ohio State University. Post that, the author worked with General Electric in divisions like Aviation, GRC and a few more for a period of 14 years. Currently working as an Associate Professor in the Department of Mechanical Engineering at IIT Patna. He has many Patents and publications in the field of gas turbines and rotor dynamics. His area of interests are rotor dynamics, gas turbine engines, friction wear, lubrication and many more.

In the current study, he has provided ideas and guidance which has led to the layout of the work presented in the paper.

Mr Anpeksh Saksena has obtained his BTech (Mechanical Engineering) from Indian Institute of Technology Patna. Currently he is pursuing his MS from Ohio State University.

In the current study, he is responsible for fabrication of Rotor rig that has been used to perform the experimentation on CSFD. Instrumentation and integration of CSFD to Jeffcott Rotor system was done by him.

Mr Aman Srivastava has obtained his BTech (Mechanical Engineering) from Indian Institute of Technology(IIT) Patna. Currently, pursuing his PhD at IIT Patna and is working in the field of non-linear dynamics. The author is also working on a project with General Electric in the Rotating Machinery Lab of IIT Patna.

In the current study, he has fabricated the ISFD using Wire-EDM which has been used to perform experimentation in this Manuscript.